THE DISTANCE-DEPENDENT TWO-POINT FUNCTION OF QUADRANGULATIONS: A NEW DERIVATION BY DIRECT RECURSION

EMMANUEL GUITTER

Abstract. We give a new derivation of the distance-dependent two-point function of planar quadrangulations by solving a new direct recursion relation for the associated slice generating functions. Our approach for both the derivation and the solution of this new recursion is in all points similar to that used recently by the author in the context of planar triangulations.

1. Introduction

The *distance-dependent two-point function* of a family of maps is, so to say, the generating function of these maps with two marked "points" (e.g. vertices or edges) at a prescribed graph distance from each other. It informs us about the distance profile between pairs of points picked at random on a random map in the ensemble at hand. In the case of planar maps, explicit expressions for the distance-dependent two-point function of a number of map families were obtained by several techniques [2, 9, 7, 1, 5, 10], all based on the relationship which exists between the two-point function and generating functions for either some particular decorated trees, or equivalently for some particular pieces of maps called *slices*. This relationship is itself a consequence of the existence of some now well-understood bijections between maps and trees or slices [14, 3].

In a recent paper [11], we revisited the distance-dependent two-point function of planar triangulations (maps whose all faces have degree 3) and showed how to obtain its expression from the solution of some direct recursion relation on the associated slice generating functions. The solution of the recursion made a crucial use of some old results by Tutte in his seminal paper [15] on triangulations. In this paper, we extend the analysis of [11] to the case of planar quadrangulations (maps which all faces of degree 4) by showing that a similar recursion may be written and solved by the same treatment as for triangulations.

The paper is organized as follows: we start in Section 2 by giving the basic definitions (Sect. 2.1) and by recalling the relation which exists between the distance-dependent two-point function of planar quadrangulations and the generating functions of particular slices (Sect. 2.2). We then derive in Section 3 a direct recursion relation for the slice generating functions, based on the definition of a particular *dividing line* drawn on the slices (Sect. 3.1) and on a decomposition of the slices along this line (Sect. 3.2). Section 4 shows how to slightly simplify the recursion by reducing the problem to slice generating functions for *simple quadrangulations*, i.e. quadrangulations without multiple edges (Sect.4.1). This allows to make the recursion relation fully tractable by giving an explicit expression for its kernel (Sects. 4.2 and 4.3). Section 5 is devoted to solving the recursion relation, first in the case of simple quadrangulations (Sect. 5.1), then for general ones (Sect. 5.2), leading eventually to some explicit expression for the distance-dependent two-point function. We conclude in Section 6 with some final remarks.

2. The two-point function and slice generating functions

2.1. **Basic definitions.** As announced, the aim of this paper is to compute the distance-dependent two-point function of planar quadrangulations. Recall that a planar map is a

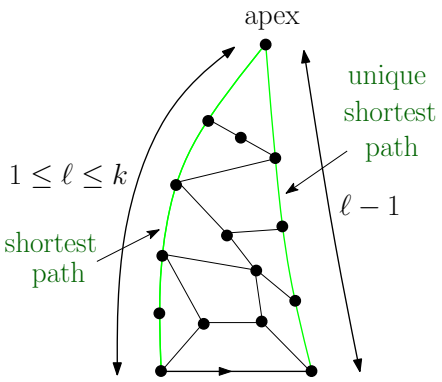

FIGURE 1. A example of slice with a boundary of length $2\ell = 10$, hence with left-boundary length $\ell = 5$, thus contributing to R_k for all $k \geq 5$.

connected graph embedded on the sphere. The map is *pointed* if it has a marked vertex (the pointed vertex) and *rooted* if it has a marked oriented edge (the root-edge). In this latter case, the origin of the root-edge is called the root-vertex. A planar quadrangulation is a planar map whose all faces have degree 4. For $k \geq 1$, we define the distance-dependent two-point function $G_k \equiv G_k(g)$ of planar quadrangulations as the generating function of pointed rooted quadrangulations whose pointed vertex and root-vertex are at graph distance k from each other. The quadrangulations are enumerated with a weight g per face. Note that, since planar quadrangulations are bipartite maps, the graph distances from a given vertex to two neighboring vertices have different parities, hence their difference is ± 1. In particular, in quadrangulations enumerated by G_k, the endpoint of the root-edge is necessarily at distance $k-1$ or $k+1$ from the pointed vertex.

A *quadrangulation with a boundary* is a rooted planar map whose all faces have degree 4, except the root-face, which is the face lying on the right of the root-edge, which has arbitrary degree. Note that this degree is necessarily even as the map is clearly bipartite. The faces different from the root-face are called *inner faces* and form the *bulk* of the map while the edges incident to the root-face (visited, say clockwise around the bulk) form the *boundary* of the map, whose *length* is the degree of the root-face.

As in [11], we may compute G_k by relating it to the generating function of *slices*, which are particular instances of quadrangulations with a boundary, characterized by the following properties: let 2ℓ ($\ell \geq 1$) be the length of the boundary, we call *apex* the vertex reached from the root-vertex by making ℓ elementary steps *along the boundary* clockwise around the bulk. The map at hand is a slice if (see figure 1):

- the graph distance from the root-vertex to the apex is ℓ. Otherwise stated, the left boundary of the slice, which is the portion (of length ℓ) of boundary between the root-vertex and the apex clockwise around the bulk is a shortest path between its endpoints within the map;
- the distance from the endpoint of the root-edge to the apex is $\ell - 1$. Otherwise stated, the right boundary of the slice, which is the portion (of length $\ell - 1$) of boundary between the endpoint of the root-edge and the apex counterclockwise around the bulk is a shortest path between its endpoints within the map;
- the right boundary is the *unique* shortest path between its endpoints within the map;
- the left and right boundaries do not meet before reaching the apex.

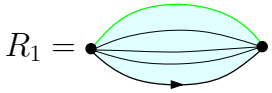

FIGURE 2. A schematic picture of a map enumerated by R_1, referred to in this paper as a *bundle* between its two boundary vertices. We indicated only those edges which connect the extremities of the root-edge to emphasize the fact that their number may be arbitrarily large.

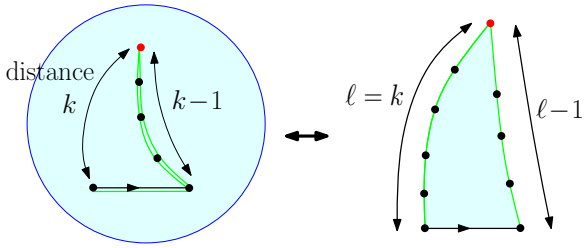

FIGURE 3. The one-to-one correspondence between pointed rooted quadrangulations whose root-edge has its extremities at respective distance k and $k-1$ from the pointed vertex (in red) and a slice with left-boundary length $\ell = k$. On the left, we have drawn (in green) the leftmost shortest paths (starting with the root-edge itself) from the the root-vertex to the pointed vertex. Cutting along this path builds the slice on the right.

We call $R_k \equiv R_k(g)$ $(k \geq 1)$ the generating function of slices with $1 \leq \ell \leq k$, enumerated with a weight g per inner face. Note that the root-edge-map, which is the map reduced to the single root-edge and a root-face of degree 2 is a slice with $\ell = 1$ and contributes a term 1 to all R_k for $k \geq 1$. The generating function R_1 deserves some special attention: by definition, R_1 enumerates slices with $\ell = 1$, hence with a boundary of length 2. The right boundary has length 0 and the apex is the endpoint of the root edge while the left boundary, of length 1, connects both extremities of the root-edge (which are necessarily distinct). This connection is also performed by the root-edge itself, and the map forms in general what we shall call a a *bundle* between the extremities of the root-edge (see figure 2). The function R_1 is thus the generating function of bundles between adjacent vertices.

2.2. **Relation between $\mathbf{G_k}$ and $\mathbf{R_k}$.** We may now easily relate G_k to R_k via the following argument: consider a pointed rooted quadrangulation enumerated by G_k. As already mentioned, the endpoint of the root-edge is necessarily at distance $k-1$ or $k+1$ from the pointed vertex, which divides the maps at hand into two categories. Assume that the map belongs to the first category, for which the distance is $k-1$. Then we may draw the *leftmost* shortest path from the root-vertex to the pointed vertex, choosing as first step the root-edge itself (see figure 3). Cutting along this shortest path creates a map with a boundary of length $2k$ which is easily seen to be a slice of left-boundary length k, which is moreover not reduced to the root-edge-map when $k = 1$. Such slices are enumerated by $R_k - R_{k-1}$ (since we must suppress from R_k the slices with $1 \leq \ell \leq k-1$) for $k \geq 2$ and by $R_1 - 1$ for $k = 1$. This yield a contribution $R_k - R_{k-1} - \delta_{k,1}$ to G_k from the first category, where we take the usual convention that $R_0 = 0$. The second category corresponds to maps whose root-edge has its endpoint at distance $k+1$ from the pointed vertex. By reversing the orientation of the root-edge, they are in bijection with maps of the first category, up to a change $k \to k+1$,

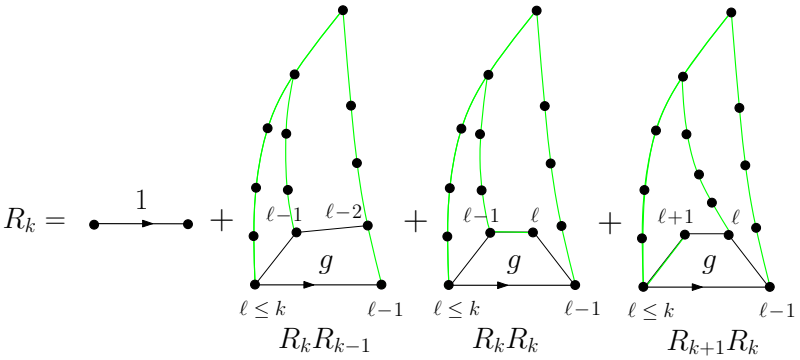

FIGURE 4. The decomposition of slices leading to eq. (2). If not reduced to the root-edge-map (weight 1), the slice with $1 \le \ell \le k$ is decomposed by removing the face immediately on the left of the root-edge (weight g), whose intermediate vertices are at distance $(\ell-1,\ell-2)$ (in which case the second vertex lies on the right boundary), $(\ell-1,\ell)$ or $(\ell+1,\ell)$. Cutting along the leftmost shortest paths from these vertices to the apex produces two sub-slices enumerated by R_kR_{k-1}, R_k^2 and R_kR_{k+1} respectively.

hence are enumerated by $R_{k+1}-R_k$ (since $\delta_{k+1,1}=0$ for $k\ge 1$). To summarize, we have the relation

$$G_k = (R_k - R_{k-1} - \delta_{k,1}) + (R_{k+1}-R_k) = R_{k+1} - R_{k-1} - \delta_{k,1}\ , \qquad k\ge 1 \tag{1}$$

which the convention $R_0=0$.

As for the slice generating functions R_k ($k\ge 1$), they satisfy the now well-known equation [2] (see below for its derivation)

$$R_k = 1 + g\, R_k(R_{k-1}+R_k+R_{k+1})\ , \qquad k\ge 1 \tag{2}$$

with $R_0=0$. In particular, it is interesting to introduce the quantity $R_\infty = \lim_{k\to\infty} R_k$ which is the generating function of slices with arbitrary left-boundary length $\ell\ge 1$. From (2), this quantity is directly obtained as the solution of

$$R_\infty = 1 + 3g\, R_\infty^2 \tag{3}$$

which satisfies $R_\infty = 1+O(g)$. Equation (2) may be viewed as a recursion on k (giving R_{k+1} from the knowledge of R_k and R_{k-1}) but this recursion requires at initial data the knowledge of R_1. In the present case, it can be shown [4] that $R_1 = R_\infty - g\, R_\infty^3$ and (2) allows one in principle to determine R_k for all k. Getting an *explicit expression* for R_k by this approach is a different story and so far, no real constructive way to solve (2) was proposed. Instead, the method used so far was to first *guess* the expression for R_k and then verify that it solves (2). This led to the explicit formula for R_k given in [2], and eventually to G_k. Another approach to determine R_k was elaborated in [7] where it was shown that the R_k's appear as coefficients in a suitable continued fraction expansion for a standard generating function of quadrangulations with a boundary. In this paper, we present a new direct recursion relation for R_k which we shall then solve explicitly in a constructive way.

To end this section, let us briefly recall for completeness the derivation of (2). Consider a map enumerated by R_k not reduced to the root-edge-map and consider the face directly on the left of the root-edge. If the left-boundary length of the slice is ℓ ($1\le\ell\le k$), the sequence of distances to the apex of the four successive vertices[1] of the face, clockwise

[1] In all generality, it may happen that the four vertices are not distinct, in which case we must more precisely consider the four successive *corners* around the face, the distance to the apex of a corner being

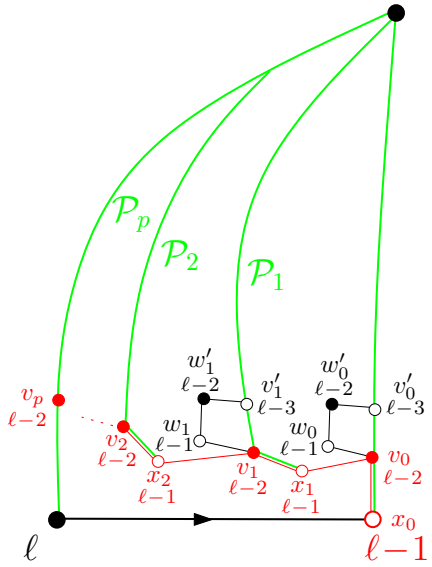

FIGURE 5. The construction of the dividing line (see text for details).

around the face starting from the root-vertex is either $\ell \to \ell-1 \to \ell-2 \to \ell-1$ (if $\ell \geq 2$), $\ell \to \ell-1 \to \ell \to \ell-1$ or $\ell \to \ell+1 \to \ell \to \ell-1$ (see figure 4). Note that each of these paths of length 3 has exactly two "descending steps" (i.e. steps for which the distance decreases by 1). We may now draw, starting from the two intermediate vertices, the leftmost shortest paths from these vertices to the apex. This divides the slice into two slices (see figure 4) whose two root-edges correspond precisely to the two descending steps. For the sequence $\ell \to \ell-1 \to \ell-2 \to \ell-1$, the respective left-boundary lengths of the two slices are ℓ' and $\ell''-1$ with $\max(\ell', \ell'') = \ell$. Demanding $\ell \leq k$ is equivalent to demanding $\ell' \leq k$ and $\ell''-1 \leq k-1$ so that the slice pairs are enumerated by $R_k\, R_{k-1}$, which explains the first of the three quadratic terms in (2). The two other terms come from the two other possible distance sequences, while the first term 1 corresponds to the edge-root-map. This explains (2).

3. A direct recursion relation for slice generating functions

3.1. **Definition of the dividing line.** We shall now derive a new direct recursion for R_k. More precisely, our recursion is best expressed in terms of the generating function

$$T_k \equiv R_k - R_1\ , \qquad k \geq 1 \tag{4}$$

which enumerates slices with left-boundary length ℓ satisfying $2 \leq \ell \leq k$ (in particular $T_1 = 0$). As in [11], our recursion is based on a decomposition of the map along a particular *dividing line* which we define now. Consider a slice with left-boundary length $\ell \geq 3$. The dividing line is a sequence of edges which are alternatively of type $\ell-2 \to \ell-1$ and $\ell-1 \to \ell-2$. It forms a simple open curve which connects the right and left boundaries of the slice, hence separates the apex from the root-vertex. To construct the line, we proceed as follows: consider the vertices v_0 and v_0' of the right boundary at respective distance $\ell-2$ and $\ell-3$ from the apex and consider the face directly on the left of the right-boundary edge linking v_0 to v_0' (see figure 5). Call w_0 and w_0' the two other vertices incident to this face (so that the sequence clockwise around the face is $v_0 \to w_0 \to w_0' \to v_0'$). The four

the distance to the apex of the incident vertex. Our statements may be straightforwardly adapted to these cases.

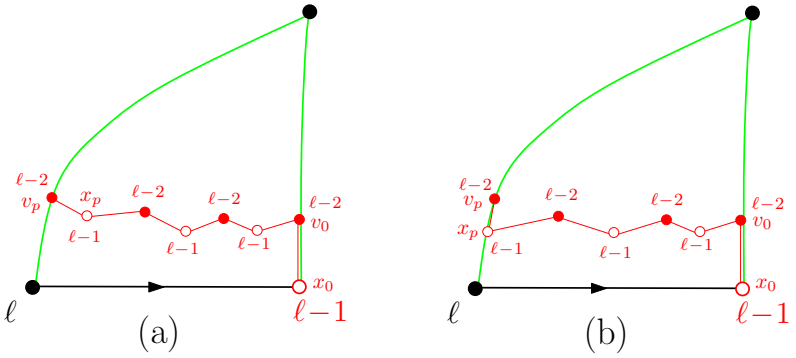

FIGURE 6. The two possible ways for the dividing line to connect to the left boundary.

vertices are necessarily distinct as otherwise, we could find a shortest path from v_0 to the apex lying strictly to the left of the right boundary, in contradiction with the fact that the right-boundary is the unique shortest path from the endpoint x_0 of the root-edge to the apex. Moreover, the distance from w_0 to the apex (which is *a priori* $\ell-3$ or $\ell-1$) cannot be equal to $\ell-3$ as this would again imply the existence of a shortest path from v_0 to the apex, hence also from x_0 to the apex, lying strictly to the left of the right boundary. The clockwise sequence of labels is thus necessarily $\ell-2 \to \ell-1 \to \ell-2 \to \ell-3$. In particular, w_0 cannot be equal to x_0 since w_0 has a neighbor at distance $\ell-2$ which does not lie on the right boundary. We conclude that there exists a path of two steps going from v_0 to a nearest neighbor w_0 at distance $\ell-1$ distinct from x_0 and then to a next-nearest neighbor w_0' at distance $\ell-2$ distinct from v_0. Let us pick the *leftmost such path of two steps*, i.e. going from v_0 to a nearest neighbor x_1 at distance $\ell-1$ distinct from x_0 and then to a next-nearest neighbor v_1 at distance $\ell-2$ distinct from v_0. We may now draw the leftmost shortest path $\mathcal{P}_1$ from x_1 to the apex, starting with the edge $x_1 \to v_1$, and call v_1' the vertex at distance $\ell-3$ along $\mathcal{P}_1$. Considering the face immediately on the left of the edge of $\mathcal{P}_1$ from v_1 to v_1', and calling w_1 and w_1' the two other incident vertices, again the four vertices v_1, w_1, w_1', v_1' around the face are necessarily distinct as otherwise, $\mathcal{P}_1$ would not be a leftmost shortest path, and, for the same reasons as above, w_1 and w_1' are necessarily at respective distances $\ell-1$ and $\ell-2$ from the apex. In particular, w_1 cannot be equal to x_1 as otherwise, x_1 would have a neighbor w_1' at distance $\ell-2$ distinct from v_0 [2] and strictly to the left of v_1, a contradiction. To summarize, this proves the existence of a path of two steps going from v_1 to a nearest neighbor at distance $\ell-1$ distinct from x_1 and then to a next-nearest neighbor at distance $\ell-2$ distinct from v_1. Again we pick the leftmost such path and call x_2 and v_2 the corresponding vertices (see figure 5), then drawn the leftmost shortest path $\mathcal{P}_2$ from x_2 to the apex (starting with the edge $x_2 \to v_2$). Continuing this way, we build by simple concatenation of the right-boundary edge from x_0 to v_0 and of all the elementary two-step paths a path connecting x_0 to v_0 to x_1 to v_1 to x_2 to v_2 and so on, where all the x_i's are at distance $\ell-1$ from the apex and all the v_i's at distance $\ell-2$. As explained below, this path *cannot form a loop* so it defines an open simple curve which necessarily reaches, after p iterations of the process ($p \geq 1$), the vertex v_p lying on the left boundary at distance $\ell-2$ from the apex: this path defines our dividing line. Note that two situations may occur according to whether x_p itself belongs to the left boundary or not (see figure 6).

By construction, the dividing line is thus a simple open curve connecting x_0 to v_p by visiting alternatively vertices at distance $\ell-1$ and $\ell-2$ from the apex. The line therefore

[2]The fact that w_1' is itself distinct from v_0 is because otherwise, the edge $w_1' \to v_1'$ would lie strictly to the left of the right boundary and connect v_0 to a vertex at distance $\ell-3$, which is forbidden.

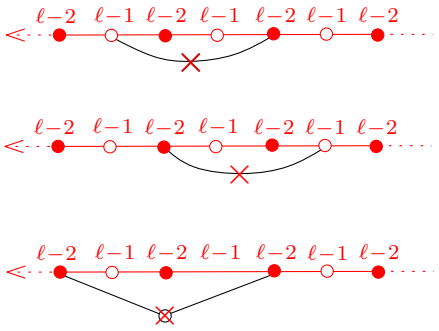

FIGURE 7. A schematic picture of the properties of the dividing line emphasized in Property 1. Vertices at distance $\ell-2$ (resp. $\ell-1$) are colored in black (resp. in white).

separates two domains in the slice, an upper part containing the apex and a lower part containing the root-vertex. Clearly, since a path from the apex to the lower part must cross the dividing line, all the the vertices strictly inside the lower part are at distance at least $\ell-1$ from the apex. By construction, the dividing line satisfies moreover the following property (illustrated in figure 7):

Property 1.

- *Two vertices of the dividing line cannot be linked by an edge lying strictly inside the lower part.*
- *Two vertices of the dividing line at distance $\ell-2$ cannot have a common neighbor strictly inside the lower part.*

The first statement is clear as the existence of an edge linking two vertices of the dividing line and inside the lower part would produce at some iteration of the dividing line construction an acceptable two-step path lying to the left of the chosen one. As for the second statement, the common vertex would necessarily be at distance $\ell-1$ and again an acceptable two-step path would lie to the left of the chosen one. Note that, by contrast, pairs of vertices of the dividing line at distance $\ell-1$ may have a common neighbor strictly inside the lower part.

The fact that the concatenation of our two-step paths cannot form a loop may be understood via arguments similar to those discussed in [11]. The proof is as follows: assume that the line forms a loop and consider the first vertex v_i, $i\geq 0$ (or respectively x_j, $j>0$) at which a double point arrises, i.e. $v_{i+m}=v_i$ for some $m>1$ (respectively $x_{j+m}=x_j$). Note that $m=1$ is not possible from our construction of the two-step paths. Note also that the connection cannot occur at x_0 as this vertex has only one neighbor, v_0, at distance $\ell-2$. If the connection occurs from the left (see figure 8), then the two-step path $v_i\to x_{i+m}\to v_{i+m-1}$ (respectively $v_{j-1}\to x_j\to v_{j+m-1}$) lies on the left of the chosen path $v_i\to x_{i+1}\to v_{i+1}$ (respectively $v_{j-1}\to x_j\to v_j$) and should thus have been chosen instead of this latter path. This is a contradiction. If the connection occurs from the right, we use the property that, by construction, each vertex v_n of the dividing line at distance $\ell-2$ from the apex has a neighbor on $\mathcal{P}_n$, therefore *on its right*, at distance $\ell-3$ from the apex (see figure 8). Then a loop closing from the right encloses at least one vertex at distance $\ell-3$ (for instance the neighbor of v_{i+m}, respectively of v_{j+m-1}) which is de facto surrounded by a frontier made of vertices at distance $\ell-2$ and $\ell-1$, a contraction. We conclude that the dividing line cannot form a loop and necessarily ends on the left boundary.

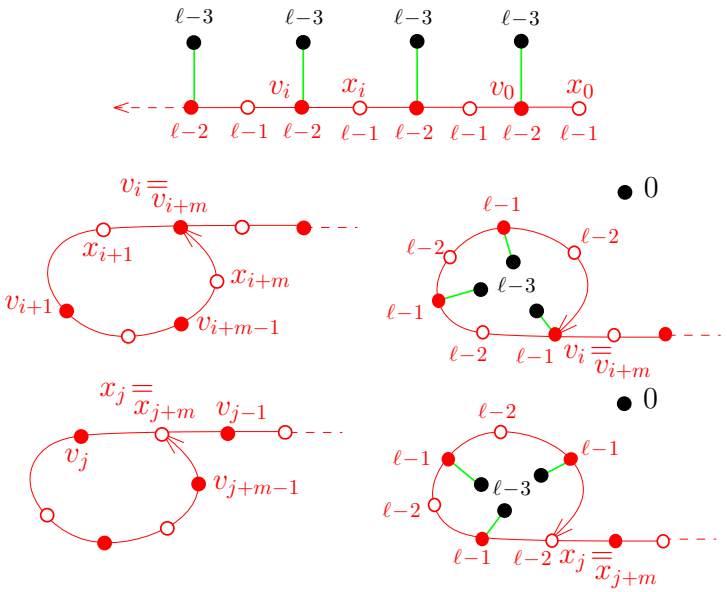

FIGURE 8. A schematic picture of the dividing line (top, in red) made of its succession of vertices x_i at distance $\ell-1$ and v_i at distance $\ell-2$, with a vertex at distance $\ell-3$ attached to the right of each v_i. The lower part of the figure illustrates the contradictions which would occur if the dividing line were making a loop (see the arguments in the text).

As a final remark, we considered so far slices whose left-boundary length ℓ satisfies $\ell \geq 3$. When dealing with T_k, we also need to consider slices with $\ell = 2$. For such slices, we define the dividing line as made of the single right-boundary edge linking the endpoint x_0 of the root-edge to the apex v_0.

3.2. **Decomposition of slices.** As in [11], the dividing line allows us to decompose slices enumerated by T_k in a way which leads to a direct recursion relating T_k to T_{k-1}. As in previous section, the sequence of vertices along the dividing line will be denoted by $(x_0, v_0, x_1, v_1, \cdots, x_p, v_p)$ with $p \geq 0$, where the vertices x_i (respectively v_i) are at distance $\ell-1$ (respectively $\ell-2$) from the apex, ℓ being the left-boundary length of the slice (and the constraint that $p = 0$ if and only if $\ell = 2$). The decomposition is as follows: as already mentioned, the dividing line separates the slice into two domains, a lower part which contains the root-vertex and a complementary upper part (empty if and only if $\ell = 2$). For $\ell \geq 3$, this upper part may be decomposed into slices by drawing the leftmost shortest path $\mathcal{P}_i$ from each vertex x_i $(0 \leq i \leq p)$ to the apex (the path starting with the edge of the dividing line linking x_i to v_i). Note that $\mathcal{P}_0$ is the right boundary while $\mathcal{P}_p$ sticks to the left boundary from v_p to the apex. The paths $\mathcal{P}_i$ decompose the upper part in p slices of left-boundary lengths between 2 and $k-1$, hence enumerated by T_{k-1}, with a slice associated to each step $v_{i-1} \to x_i$ $(1 \leq i \leq p)$ along the dividing line (the root-edge of this slice being the edge of the dividing line linking v_{i-1} to x_i, oriented from x_i to v_{i-1} – se figure 9).

More interesting is the decomposition of the lower part. We start by looking at the connections of the root-vertex to the dividing line: the root vertex, at distance ℓ from the apex, is, in all generality, adjacent to a number of vertices x_i of the dividing line. These include x_0 plus possibly a number of other x_i's, for instance x_p in the situation (b) of figure 6. Note that these connections are in general achieved by a bundle (whose boundary if formed by the extremal edges performing the connection from the root-vertex to x_i). Now

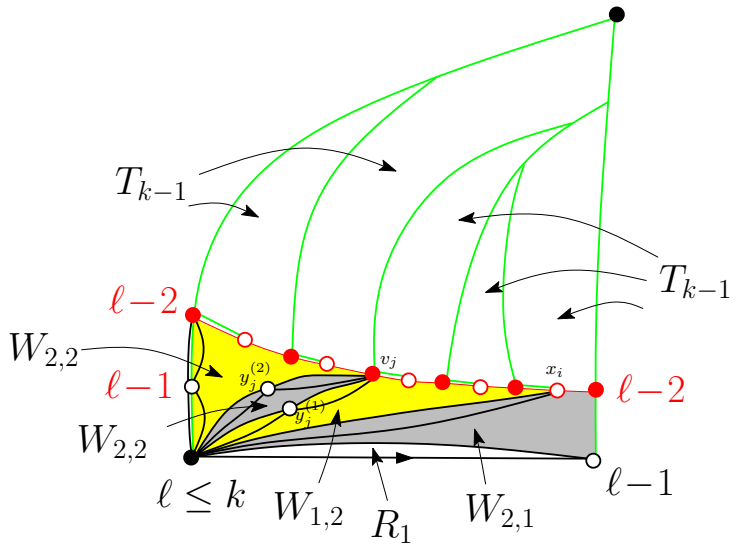

FIGURE 9. The decomposition of a slice on both sides of the dividing line (see text). In the upper part, a slice enumerated by T_{k-1} is created for each black-white edge of the dividing line (represented in red, supposedly oriented toward the left - here black and white vertices are represented by filled or empty red circles). In the lower part, a first bundle (enumerated by R_1) between the extremities of the root-edge is completed by a sequence of blocks (here represented alternatively in grey and yellow). Each block has its right and left frontiers of lengths 1 or 2 and is enumerated by $W_{1,1}$, $W_{1,2}$, $W_{2,1}$ or $W_{2,2}$ accordingly. In the present illustration, we have one $(2,1)$ block, one $(1,2)$ block and two $(2,2)$ blocks.

the root-vertex is also in all generality, connected to a number of vertices v_j of the dividing line by two-step paths whose intermediate vertex y_j lies strictly inside the lower domain (and is at distance $\ell-1$ from the apex). These include for instance v_p in the situation (a) of figure 6. The connection from the root-vertex to y_j and from y_j to v_j is achieved in general by a *pair of bundles*. Moreover several intermediate vertices $y_j^{(1)}, y_j^{(2)}, \cdots, y_j^{(m)}$ may exist for the same v_j (see figure 9). Now for each connection from the root-vertex to some x_i, we cut along the *leftmost* edge performing this connection and for each two-step-path connection from the root-vertex to some v_j via some y_j, we cut along the *leftmost* two-step path performing the connection. If several intermediate vertices $y_j^{(1)}, y_j^{(2)}, \cdots, y_j^{(m)}$ exist, we make one cut for *each occurrence* of such a vertex (see figure 9). These cuts divide the lower part into a sequence of connected domains whose left and right frontiers correspond to the performed cuts and have length 1 if the corresponding cut leads to some x_i or 2 if the corresponding cut leads to some v_j. The domains may thus be classified in four categories: $(1,1)$, $(1,2)$, $(2,1)$ or $(2,2)$ according to their right- and left-frontier length respectively (for instance, the type $(1,2)$ corresponds to a right-frontier length 1 and a left-frontier length 2). To be precise, the decomposition of the lower part may be characterized by some sequence $a_0, a_1, \cdots, a_n$, $n \ge 1$ (with $a_i, \in \{1,2\}$) corresponding to the successive encountered frontier lengths for the cut domains. To each elementary step $a_i \to a_{i+1}$ of the sequence is attached a block of type (a_i, a_{i+1}).

The beginning of the sequence requires some special attention. Indeed, in the cutting, a first bundle from the root-vertex to x_0 is delimited, enumerated by R_1 (see figure 9), Ignoring

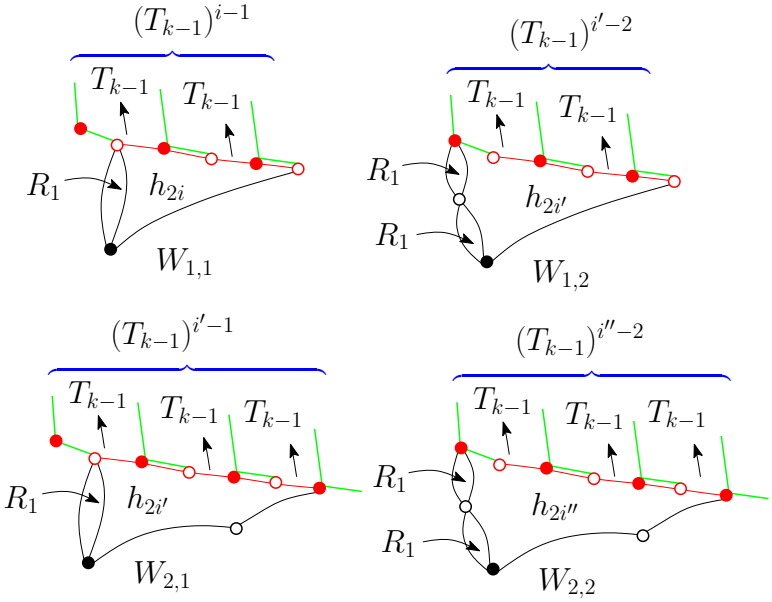

FIGURE 10. Computation of the weights $W_{1,1}$, $W_{1,2}$, $W_{2,1}$ and $W_{2,2}$. For instance, the top-left situation corresponds to maps enumerated by $W_{1,1}$ for which we may extract a bundle (enumerated by R_1) along the left frontier. The remaining part, of length $2i$ (here $i=3$) is enumerated by h_{2i} and gives rise to $i-1$ black-white (from right to left) edges on the dividing line, hence $i-1$ factors T_{k-1}. The other situations are represented with $i'=4$ (for $W_{1,2}$, and $W_{2,1}$) and $i''=5$ (for $W_{2,2}$).

this first bundle, the effective right frontier of the first block is therefore a two-step path from the root-vertex to $y_0=x_0$, then to v_0. We thus should start our sequence with $a_0=2$ (note that the root vertex may be also connected to v_0 by two-step paths lying strictly inside the lower part, in which case $a_1=2$ too). The sequence ends either with $a_n=2$ if the dividing line is in the situation (a) of figure 6 or with $a_n=1$ if the dividing line is in the situation (b) of figure 6.

Let us now discuss the weight that should be attached to each block of the sequence if we wish to compute T_k. Consider first a block of type $(1,1)$ (see figure 10): it has an overall boundary of length $2i\geq 4$ made of its right frontier (a single edge of length 1), its left frontier (a single edge of length 1 which is in general the leftmost edge of a bundle) and a portion of length $2i-2$ of the dividing line which goes from some x_j to x_{j+i-1}, hence contains $i-1$ edges of type $v_m\to x_{m+1}$, giving rise to $i-1$ slices in the upper part, hence producing a weight T_{k-1}^{i-1}. As for the block itself in the lower part, we may decide to cut out the bundle to which belongs the left frontier of the block, giving rise to a weight R_1. The remaining part (which has now as left frontier the rightmost edge of the bundle) is enumerated by some generating function $h_{2i}=h_{2i}(g)$ for particular quadrangulations with a boundary of length $2i$ satisfying special constraints which we will discuss below (see Property 2). At this stage, let us just mention that we decide to choose as root-edge for these quadrangulation the edge starting from the root-vertex counterclockwise around the domain.

To summarize, the weight attached to a $(1,1)$ block is

$$W_{1,1}=R_1\sum_{i\geq 2} h_{2i}\,T_{k-1}^{i-1}\ .$$

If we now consider a block of type $(1,2)$ of the lower domain, it has an overall boundary of length $2i \geq 4$ made of its right frontier (a single edge of length 1), its left frontier (a two-step path of length 2 which is in general part of a pair of bundles) a portion of length $2i-3$ of the dividing line which goes from some x_j to v_{j+i-2}, hence contains $i-2$ edges of type $v_m \to x_{m+1}$, giving rise to $i-2$ slices in the upper domain, hence a weight T_{k-1}^{i-2}. As for the part in the lower domain, we again decide to cut out the pair of bundles to which belongs the left frontier of the block, giving rise to a weight R_1^2. The remaining part is again enumerated by h_{2i} since the remaining quadrangulation of boundary length i is precisely of the same type as above. The weight attached to a $(1,2)$ block is therefore

$$W_{1,1} = R_1^2 \sum_{i\geq 2} h_{2i}\, T_{k-1}^{i-2} \ .$$

Repeating the argument for $(2,1)$ and $(2,2)$ blocks, we find (see figure 10)

$$W_{2,1} = W_{1,1} \qquad W_{2,2} = W_{1,2} \ ,$$

so that $W_{a,a'}$ actually depends only on the second index a' (this is because both the number of bundles on the left side of the block and the number of created slices in the upper part for a fixed i depend only on a' – see figure 10). To get T_k, we must sum over all possible sequences $a_0, a_1, \cdots, a_n$. Since $a_0 = 2$ is fixed and all the other a_i's are free (including a_n) and since the weights $W_{a,a'}$ depends only on a', we immediately deduce the contribution

$$R_1 \sum_{\substack{a_0=2 \\ a_1,\cdots,a_n\in\{1,2\}}} \prod_{i=0}^{n-1} W_{a_i,a_{i+1}} = R_1 \left(R_1 \sum_{i\geq 2} h_{2i}\, T_{k-1}^{i-1} + R_1^2 \sum_{i\geq 2} h_{2i}\, T_{k-1}^{i-2} \right)^n$$

for a sequence of length n, where we re-introduced the weight R_1 for the bundle from the root-vertex to x_0. Recall that $n \geq 1$ since we have at least one block. Note also that slices with $\ell = 2$ contribute to all values of n via the $i = 2$ term of the second sum in the parenthesis above[3].

Summing over all $n \geq 1$, we arrive at the desired recursion relation

$$T_k = \frac{R_1 \left(R_1 \sum_{i\geq 2} h_{2i}\, T_{k-1}^{i-1} + R_1^2 \sum_{i\geq 2} h_{2i}\, T_{k-1}^{i-2} \right)}{1 - \left(R_1 \sum_{i\geq 2} h_{2i}\, T_{k-1}^{i-1} + R_1^2 \sum_{i\geq 2} h_{2i}\, T_{k-1}^{i-2} \right)}$$

or in short

$$T_k = \frac{R_1^2 (T_{k-1} + R_1)\, \Phi(T_{k-1})}{1 - R_1 (T_{k-1} + R_1)\, \Phi(T_{k-1})} \ , \qquad \Phi(T) \equiv \Phi(T,g) = \sum_{i\geq 2} h_{2i}(g)\, T^{i-2} \ . \tag{5}$$

To end the section, it remains to characterize the quadrangulations with a boundary of length $2i$ ($i \geq 2$) enumerated by $h_{2i} \equiv h_{2i}(g)$, where g is the weight per face. By construction, the boundary of these quadrangulations is a simple curve and we may for convenience decide to color the boundary vertices alternatively in black and white, the root-vertex being black (thus the v_i's at hand are also black and the x_j and $y_j^{(\alpha)}$ are white). The maps enumerated by h_{2i} are further characterized by the following property (see figure 11):

Property 2.

- *In the maps enumerated by h_{2i}, two vertices of the boundary cannot be linked by an edge lying strictly inside the map.*
- *In the maps enumerated by h_{2i}, two black vertices of the boundary cannot have a common (white) adjadent vertex strictly inside the map.*

[3]For $\ell = 2$, we have $a_i = 2$ for all i ($0 \leq i \leq n$) and all the blocks have boundary length 4, hence are enumerated by $R_1^2\, h_4$. In particular with have $T_2 = R_1 \sum_{n\geq 1} (R_1^2 h_4)^n = R_1^3\, h_4/(1 - R_1^2\, h_4)$, in agreement with (5) for $k = 2$, since $T_1 = 0$ and $\Phi(0) = h_4$.

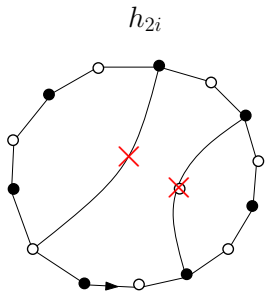

FIGURE 11. A schematic representation of the two forbidden connections within maps enumerated by h_{2i}, as dictated by Property 2.

For pairs of vertices belonging to the dividing line, these properties are a direct consequence of Property 1. For pairs involving the other vertices (i.e. the root vertex or the intermediate vertices y_j), these properties are a direct consequence of the block decomposition. As in [11], it is remarkable that, while, in the decomposition, boundary vertices of the domains enumerated by h_{2i} play different roles, the characterization of these domains via Property 2 turns out to be symmetric for all boundary vertices.

4. Simple quadrangulations

4.1. **From general to simple quadrangulations.** As in [11], we may slightly simplify our recursion by eliminating R_1 from our problem. At the level of maps, it amounts to restrict our analysis to *simple* quadrangulations (with a boundary), i.e. quadrangulations *without multiple edges*. We thus define simple analogs of R_k and T_k, namely the generating function $r_k \equiv r_k(G)$ of simple slices with left-boundary length ℓ in the range $1 \leq \ell \leq k$ and $t_k \equiv t_k(G)$ for simple slices with $2 \leq \ell \leq k$, with a weight G per inner face. Similarly, we define $\tilde{h}_{2i} \equiv \tilde{h}_{2i}(G)$ as the generating function, with a weight G per inner face, of simple quadrangulations with a boundary of length $2i$ forming a simple curve (i.e. which does not cross itself), and which satisfy Property 2. As it is well-known, we may pass from simple quadrangulations to general quadrangulations by a substitution in the generating functions. Indeed, a general quadrangulation is obtained from a simple one by replacing each edge of the simple quadrangulation by a bundle, as we defined it. Since the generating function for bundles is R_1, the generating functions R_k, T_k, and h_{2i} may in practice be obtained from r_k, t_k, and $\tilde{h}_{2i}$ by a substitution as follows: consider a quandrangulation with F inner faces, E inner edges and $2L$ edges on the boundary. We have the relation $4F = 2E + 2L$ so that

$$E = 2F - L \ .$$

In the case of maps enumerated by R_k (respectively T_k), we must, starting from maps enumerated by r_k (respectively t_k), put a weight R_1 to each inner edge as well as to each of the $L = \ell$ edges of the left boundary and finally to the root edge. No weight R_1 is assigned to the edges of the right boundary as bundles cannot be present there since the right boundary is the unique shortest path between its extremities. We must thus assign a global weight $R_1^{E+L+1} = R_1 \times R_1^{2F}$ (note that, written this way, the weight is independent of ℓ). In other words, we must assign a weight R_1^2 per face and a global factor R_1, which yields the relations

$$R_k(g) = R_1\, r_k(G) \ , \qquad T_k(g) = R_1\, t_k(G) \ , \tag{6}$$

with the correspondence

$$G = g\, R_1^2 \ . \tag{7}$$

Note that the relation $T_k = R_k - R_1$ translates into

$$t_k = r_k - 1$$

consistent with the fact that there is a unique simple slice with $\ell = 1$, the root-edge-map, hence $r_1 = 1$. As for h_{2i}, it is obtained by assigning a weight R_1 to all the inner edges of the maps enumerated by $\tilde{h}_{2i}$. Again, because of Property 2, there cannot be multiple edges on the boundary. We must thus assign a global weight $R_1^E = R_1^{2F-L} = R_1^{2F-i}$ since $L = i$ in this case. In other word, we must again assign an extra weight R_1^2 per face and now a global factor R_1^{-i}, which yields

$$h_{2i}(g) = R_1^{-i}\, \tilde{h}_{2i}(G) \tag{8}$$

with the correspondence (7). Introducing the quantity

$$\tilde{\Phi}(t) \equiv \tilde{\Phi}(t, G) = \sum_{i \geq 2} \tilde{h}_{2i}(G)\, t^{i-2} \ , \tag{9}$$

we deduce from (8)

$$\Phi(T) = R_1^{-2}\, \tilde{\Phi}(t) \ , \qquad T = R_1\, t$$

with the implicit correspondence (7).

Finally, the recursion (5) translates into the simpler relation

$$t_k = \frac{(t_{k-1}+1)\, \tilde{\Phi}(t_{k-1})}{1 - (t_{k-1}+1)\, \tilde{\Phi}(t_{k-1})} \tag{10}$$

(with $t_1 = 0$) where, as promised, R_1 is no longer present. As in [11], we note that there is no straightforward analog of the relation (1) for simple quadrangulations. This is because closing a slice into a planar quadrangulations by identifying its right and left boundaries as in figure 3 may in general create multiple edges. The recourse to simple slices in this paper should therefore simply be viewed as a non-essential but convenient way to slightly simplify our recursion by temporarily removing the R_1 factors.

4.2. **An equation for $\tilde{\mathbf{\Phi}}(\mathbf{t})$.** In order to solve (10), and eventually (5), we need some more explicit expression for $\tilde{\Phi}(t)$. Such expression may be obtained by first noting that $\tilde{\Phi}(t)$ is fully determined by the following equation:

$$\tilde{\Phi}(t) = G + \frac{G}{t} \left\{ \frac{(t+1)\tilde{\Phi}(t)}{1 - (t+1)\tilde{\Phi}(t)} - \frac{\tilde{h}_4}{1 - \tilde{h}_4} \right\} \tag{11}$$

which may equivalently be written as

$$t(1+t)\tilde{\Phi}^2(t) + (G(1+t)(1-t+g_4) - t)\, \tilde{\Phi}(t) + G(t - g_4) = 0 \ , \qquad g_4 \equiv \frac{\tilde{h}_4}{1 - \tilde{h}_4} \ .$$

Let us first prove (11) and then show how to get $\tilde{\Phi}(t)$ out of it. From the definition (9), $t^2\, \tilde{\Phi}(t)$ enumerates simple quandrangulations with a boundary of *arbitrary length* $2i$ ($i \geq 2$) forming a simple curve and satisfying Property 2, with a weight G per inner face and a weight $\sqrt{t}$ per boundary edge. The quadrangulation may be reduced to a single face (with a boundary of length 4), leading to a first contribution $t^2\, G$ to $t^2\, \tilde{\Phi}(t)$, hence (after dividing by t^2) to the first term in (11). In all the other cases, we may look at the face immediately on the left of the root-edge and call v and w its black and white incident vertices other than the extremities of the root-edge (recall that we decided for convenience to bi-color the map in black and white, the root-vertex being black). The (black) vertex v *cannot lie on the boundary* as otherwise, w (which could not lie in this case on the boundary because of the first requirement of Property 2) would be a common neighbor to v and to the root-vertex, thus violating the second requirement of Property 2. So v lies strictly inside the map. As for the (white) vertex w, it may lie on the boundary (see figure 12-case (a)) or not (case

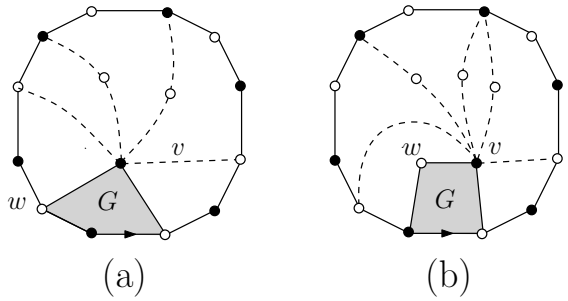

FIGURE 12. The decomposition of a map enumerated by $\tilde{\Phi}(t)$ (and not reduced to a single face). The map is decomposed by removing the face (in gray – weight G) on the left of the root-edge and cutting along all the connections of the black vertex v (incident to the gray face and strictly inside the map) to boundary vertices by either simple edges or by two-step paths. The white vertex w (incident to the gray face and different from the root-edge extremities) may lie on the boundary (case (a)) or not (case (b)). In this latter case, it cannot be connected to other black boundary vertices than the root-vertex.

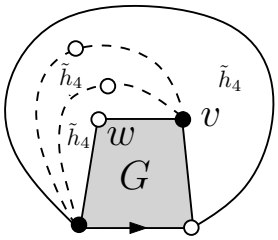

FIGURE 13. A schematic picture of those maps which have the structure of figure 12 but which do not contribute to $\tilde{\Phi}(t)$ since their boundary length is 2 (hence less than 4).

(b)). In this latter case, *w cannot be connected to a vertex of the boundary* other than the root-vertex as otherwise, the second requirement of Property 2 would again be violated. On the other hand, the vertex v is connected by simple edges to a number of white vertices of the boundary (including the endpoint of the root-edge as well as w in case (a)), and may be connected by two-step paths to black vertices of the boundary (including the root-vertex in case (b)). Let us draw all these connections and cut the map along them. After cutting, the face to the left of the root edge gets disconnected and contributes a weight $t\,G$ to $t^2\,\tilde{\Phi}(t)$ in case (a) and a weight $\sqrt{t}\,G$ in case (b). The rest of the map forms a sequence of blocks. As we did before in the slice decomposition, we may consider the sequence $a_0, a_1, \cdots, a_n$ ($n \geq 1$) of the lengths 1 or 2 of the (counterclockwise) successive connections of v to boundary vertices (with 1 for a simple edge connection to a white vertex and 2 for a two-step-path connection to a black vertex). We have $a_0 = 1$ since the first connection is from v to the white endpoint of the root-edge while $a_n = 1$ in case (a) and $a_n = 2$ in case (b). Now the m-th block has a boundary of total arbitrary length $2j$ for some $j \geq 2$, with $2j - a_{m-1} - a_m$ edges on the original boundary of the map. It must thus be given a weight $w(a_{m-1}, a_m)$ with

$$w(a, a') = \sum_{j \geq 2} \tilde{h}_{2j} (\sqrt{t})^{2j-a-a'} = (\sqrt{t})^{4-a-a'}\,\tilde{\Phi}(t)$$

Considering both cases (a) and (b), the contribution to $t^2\,\tilde\Phi(t)$ of sequences of n blocks (together with that of the face on the left of the root-edge) is therefore

$$\begin{aligned}
&\Big(\tilde\Phi(t)\Big)^n \left(\sum_{\substack{a_0=1,a_n=1\\ a_2,\cdots,a_{n-1}\in\{1,2\}}} t\,G \prod_{m=1}^{n} (\sqrt{t})^{4-a_{m-1}-a_m} \quad + \sum_{\substack{a_0=1,a_n=2\\ a_2,\cdots,a_{n-1}\in\{1,2\}}} \sqrt{t}\,G \prod_{m=1}^{n} (\sqrt{t})^{4-a_{m-1}-a_m} \right)\\
&= t\,G\,\Big(\tilde\Phi(t)\Big)^n \left(\sum_{\substack{a_n=1\\ a_2,\cdots,a_{n-1}\in\{1,2\}}} \prod_{m=1}^{n} t^{2-a_m} \quad + \sum_{\substack{a_n=2\\ a_2,\cdots,a_{n-1}\in\{1,2\}}} \prod_{m=1}^{n} t^{2-a_m} \right)\\
&= t\,G\,\Big(\tilde\Phi(t)\Big)^n \sum_{a_1,a_2,\cdots,a_n\in\{1,2\}} \prod_{m=1}^{n} t^{2-a_m}\\
&= t\,G\,\Big(\tilde\Phi(t)\Big)^n (t+1)^n\ .
\end{aligned}$$

To go from the first to the second line, we simply use the fact that $a_0 = a_n$ for sequences of the first sum and $a_0 = a_n - 1$ for sequences of the second sum. Summing over $n \geq 1$ yields the contribution

$$t\,G\,\frac{(t+1)\tilde\Phi(t)}{1-(t+1)\tilde\Phi(t)} \tag{12}$$

to $t^2\,\tilde\Phi(t)$, hence (after dividing by t^2) to the second term in (11). So far in our decomposition, we did not enforce the condition that, in $\tilde\Phi(t)$, the length $2i$ of the maps must satisfy $i \geq 2$. In our block sequences, there is a situation where this length happens to be 2 (i.e. $i = 1$) (see figure 13): it corresponds to a situation of case (b) with a first block of boundary length 4 whose boundary vertices are v, w and the two extremities of the root-edge (and with exactly 1 edge on the original boundary of the whole map), completed by arbitrarily many blocks of size 4 whose boundaries are made of two-step-paths from v to the root-vertex (these blocks do not contribute to the original boundary length). These maps, made of $n \geq 1$ blocks enumerated by $\tilde h_4$ contribute

$$t\,G \sum_{n\geq 1} (\tilde h_4)^n = t\,G\,\frac{\tilde h_4}{1-\tilde h_4}$$

to (12) and must be subtracted to properly recover $t^2\,\tilde\Phi(t)$. This explains (after dividing by t^2) the third term in (11).

4.3. **An expression for $\tilde\Phi(t)$.** We shall now extract from (11) a tractable expression for $\tilde\Phi(t)$. The first step consists in getting from the equation an expression for $\tilde h_4 = \tilde h_4(G)$ as a function of the face weight G. Here we use the following standard trick: from (11), we may write

$$\tilde h_4 = \frac{t(t+1)\tilde\Phi^2(t) - (G(t+1)(t-1)+t)\tilde\Phi(t) + G\,t}{t(t+1)\tilde\Phi^2(t) - (G(t+1)t+t)\tilde\Phi(t) + G\,(t+1)} \tag{13}$$

which, upon differentiating with respect to t (recall that $\tilde h_4$ does not depend on t), yields

$$\begin{aligned}
0 &= \frac{d\tilde h_4}{dt}\\
&\Rightarrow 0 = \tilde\Phi'(t)\left\{ t\left((t+1)^2\tilde\Phi^2(t) - 2(t+1)\tilde\Phi(t) + 1 - G\right) - G \right\}\\
&\quad + \left\{ \tilde\Phi(t)\left((t+1)^2\tilde\Phi^2(t) - 2(t+1)\tilde\Phi(t) + 1 - G\right) - G\left(1-(t+1)\tilde\Phi(t)\right)^2 \right\}\ .
\end{aligned}$$

This equation is satisfied in particular if we let t vary on a line $t=t(G)$ where each of the two terms between brackets in the above expression vanishes. Canceling these two terms and solving for G and $\tilde{\Phi}$ yields the following two possible solutions

$$G=\frac{t(G)}{(1+t(G))^3} \qquad \text{and} \qquad \tilde{\Phi}(t(G))=\frac{t(G)}{(1+t(G))^2}$$

or

$$G=\frac{1}{t(G)(1+t(G))} \qquad \text{and} \qquad \tilde{\Phi}(t(G))=\frac{1}{t(G)}$$

which select two lines $t=t(G)$ where we know the value of $\tilde{\Phi}$. Plugging these values in (13) yields

$$\tilde{h}_4=\frac{t(G)(1-t(G))}{1+t(G)-t(G)^2}$$

for the first choice and $\tilde{h}_4=1+G$ for the second choice. This latter result is clearly not satisfactory (recall that $\tilde{h}_4$ enumerates simple quandrangulations with a boundary of length 4 satisfying Property 2, with a weight G per face) so we are left with the first choice. In other words we deduce from our particular solution the parametric expression for $\tilde{h}_4$:

$$\tilde{h}_4=\frac{C(1-C)}{1+C-C^2}\ , \qquad \text{where } G=\frac{C}{(1+C)^3} \tag{14}$$

(here $C=t(G)$ should be viewed as a simple parametrization of G) which implicitly determines $\tilde{h}_4$ as a function of G.

Inverting the relation between G and C, we get

$$C=\sum_{n\geq 1}\frac{1}{2n+1}\binom{3n}{n}G^n\ . \tag{15}$$

Note that we implicitly assume that $0\leq G\leq 4/27$ for C to be well-defined as above, which in turns implies that C lies in the range $0\leq C\leq 1/2$. This is consistent with the fact that the number of simple quandrangulations grows exponentially with the number F of faces as $(27/4)^F$ [8]. Now a Lagrange inversion yields the following formula

$$[G^p]\tilde{h}_4=\sum_{n=0}^{p-1}\left(\frac{(-1)^n\omega^{n+2}-\omega^{-n-2}}{\sqrt{5}}\right)\frac{(n+1)(3p)!}{p(p-1-n)!(2p+1+n)!}\ , \qquad \omega=\frac{1+\sqrt{5}}{2}$$

(involving Fibonacci numbers) for the number of simple quandrangulations with a boundary of length 4, with p inner faces, satisfying Property 2. The first terms of this expansion read

$$\tilde{h}_4=G+G^2+3G^3+11G^4+46G^5+209G^6+\cdots \tag{16}$$

with coefficients which may easily be verified by direct inspections of the maps at hand. (see figure 14). This sequence appears in [13] in the context of the enumeration of naturally embedded ternary trees. This should not come as a surprise since bijections exist between such trees and simple quadrangulations [12, 6].

With the parametrization (14), equation (11) may be rewritten as a quadratic equation

$$\begin{aligned} t(t+1)(1+C)^3\tilde{\Phi}^2(t)+\left\{C(1+C-C^2)-t(1+3C+2C^2+2C^3)-t^2\,C\right\}\tilde{\Phi}(t) \\ +C(t-C+C^2)=0 \end{aligned} \tag{17}$$

whose discriminant reads

$$\Delta=(C-t)^2\left\{(1+C^2-C(t-1))^2-4C^2(1+C)(t+1)\right\}\ .$$

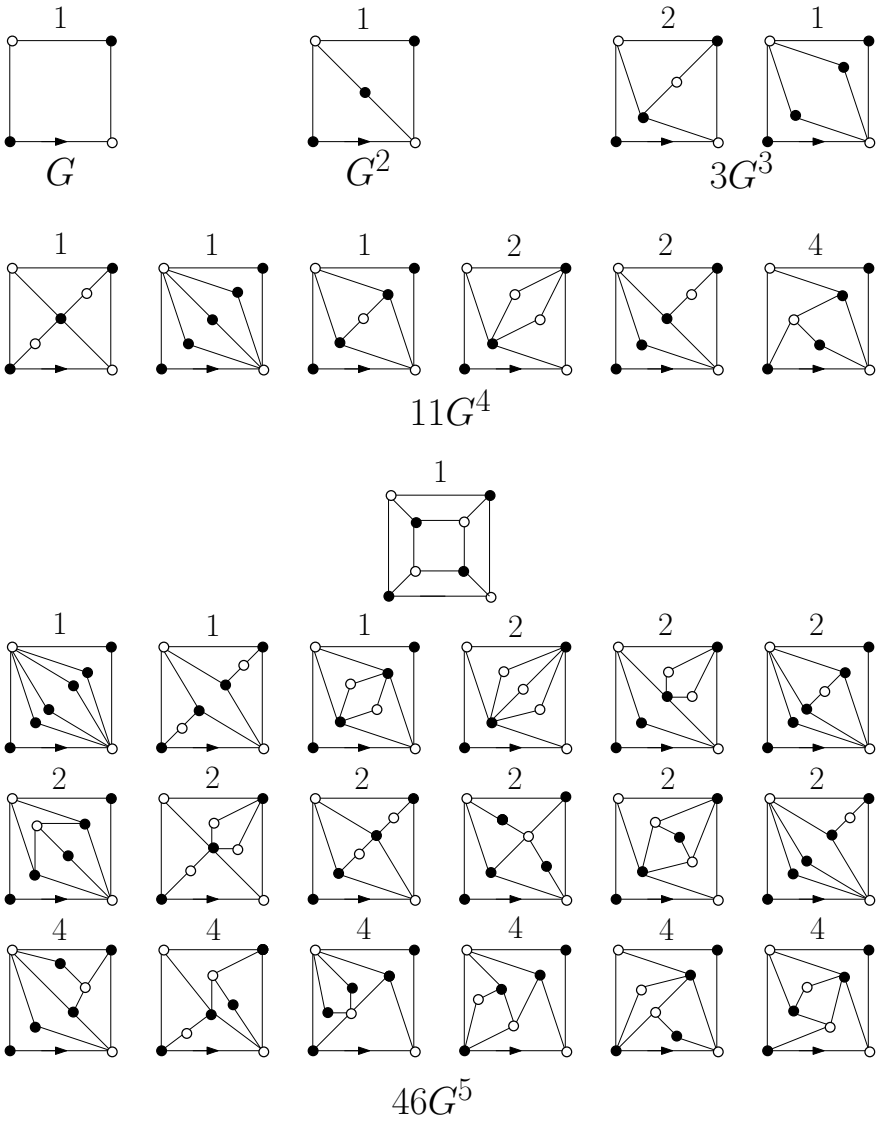

FIGURE 14. A direct inspection of the maps enumerated by $\tilde{h}_4$ and with up to 5 inner faces. To obtain all the acceptable maps, each of the maps presented here must also be reflected along its two diagonals (and re-rooted at its bottom edge). According to the symmetry of the map at hand, the number of *distinct* maps obtained by these reflections is 1, 2 or 4 as indicated. Summing these numbers yields respectively $1, 1, 3, 11$ and 46 distinct maps with $1, 2, 3, 4$ and 5 inner faces, explaining the first five terms of (16).

A look at the second factor suggests introducing the quantity[4] $Y(t)$, solution of

$$Y^2(t) + (1 + C^2 - C(t-1))\, Y(t) + C^2(1+C)(t+1) = 0 \tag{18}$$

[4]Here we use a trick in all points similar to that used by Tutte in [15].

whose two solutions $Y_\pm(t)$ are related by the following involution (obtained by eliminating t between the equation (18) for $Y(t)=Y_+(t)$ and the same equation for $Y(t)=Y_-(t)$):

$$Y_\pm(t)=\frac{C(1+C)((1+C)^2+Y_\mp(t))}{Y_\mp(t)-C(1+C)}\ . \tag{19}$$

For both determinations, we have the relation (directly read off (18)):

$$t=\frac{(1+C+Y(t))(C^2+Y(t))}{C(Y(t)-C-C^2)}\ . \tag{20}$$

Plugging this value in (17) allows to rewrite the equation for $\tilde\Phi(t)$ as

$$\left(\tilde\Phi(t)-\frac{C(1+C+C^2+Y(t))}{(1+C+Y(t))((1+C)^2+Y(t))}\right)\\ \times\left(\tilde\Phi(t)-\frac{C(Y(t)-C(1+C))(Y(t)+C^2(1+C))}{(1+C)^3Y(t)(C^2+Y(t))}\right)=0\ .$$

This gives a priori two possible expressions for $\tilde\Phi(t)$ as a function of $Y(t)$ but it is easily seen that the two formulas get interchanged by the involution (19). We may therefore decide to choose the expression coming from the first factor, namely

$$\tilde\Phi(t)=\frac{C(1+C-C^2+Y(t))}{(1+C+Y(t))((1+C)^2+Y(t))} \tag{21}$$

provided we pick the correct determination of $Y(t)$. This determination is fixed by the small t behavior $\tilde\Phi(t)=\tilde h_4+O(t)$ with the formula (14) for $\tilde h_4$. This selects the determination (recall that $0\le C\le 1/2$)

$$Y(t)=\frac{1}{2}\left\{C(t-1)-1-C^2+\sqrt{(1+C^2-C(t-1))^2-4C^2(1+C)(t+1)}\right\} \tag{22}$$

(indeed, we then have $Y(0)=-C^2$ and we recover for $\tilde\Phi(0)$ the correct expression (14) for $\tilde h_4$ while the other determination would yield $Y(0)=-C-1$ in which case $\tilde\Phi(t)$ would diverge for $t\to 0$).

Finally, from (20), the expression (21) may be simplified into

$$\tilde\Phi(t)=\frac{C^2}{Y(t)(1+C+Y(t))}+\frac{1}{t+1}\ . \tag{23}$$

Equations (23), (22) and (15), which implicitly fix $\tilde\Phi(t)=\tilde\Phi(t,G)$ in terms of G, are very reminiscent of similar expressions for triangulations (see [15, 11])

5. Solution of the recursion

5.1. **Solution for simple quadrangulations.** We are now ready to solve (10). Again, as in [11], the idea is to rewrite this recursion in terms of the variable $Y(t)$. More precisely, let us define

$$Y_k\equiv Y(t_k)\ ,\qquad \tilde\Phi_k\equiv\tilde\Phi(t_k)\ .$$

From (20), we have the relations

$$t_k=\frac{(1+C+Y_k)(C^2+Y_k)}{C(Y_k-C-C^2)}\ ,\qquad t_{k-1}=\frac{(1+C+Y_{k-1})(C^2+Y_{k-1})}{C(Y_{k-1}-C-C^2)}\ . \tag{24}$$

Our recursion (10) reads

$$t_k=\frac{(t_{k-1}+1)\,\tilde\Phi_{k-1}}{1-(t_{k-1}+1)\,\tilde\Phi_{k-1}} \tag{25}$$

with, from (23),

$$\tilde{\Phi}_{k-1} = \frac{C^2}{Y_{k-1}(1+C+Y_{k-1})} + \frac{1}{t_{k-1}+1} \ .$$

Inserting this expression in (25) and plugging the value (24) of t_{k-1}, we obtain t_k as a function of Y_{k-1}, namely:

$$t_k = \frac{Y_{k-1}(C^2-C-1-Y_{k-1})}{C((1+C)^2+Y_{k-1})} \ .$$

Equating this formula with that of (24) for t_k, we obtain the following relation between Y_k and Y_{k-1}:

$$(1+C+Y_{k-1}+Y_k)\left(C^2(1+C)^2 - C(1+C)Y_{k-1} + (1+C)^2 Y_k + Y_{k-1}Y_k\right) = 0 \ .$$

To choose which factor to cancel, we note that, for $G \to 0$, t_k and t_{k-1} tend to 0 and thus Y_k and Y_{k-1} tend to $-C^2 \to 0$ so the first factor does not vanish. The correct choice is therefore to cancel the second factor and we arrive at the remarkably simple recursion relation for Y_k:

$$Y_k = \frac{C(1+C)\,Y_{k-1} - C^2(1+C)^2}{Y_{k-1} + (1+C)^2} \ . \tag{26}$$

As recalled in [11], solving such a recursion relation is a standard exercise. To solve more generally the equation

$$Y_k = f(Y_{k-1}) \ , \qquad f(Y) \equiv \frac{a\,Y+b}{c\,Y+d} \ ,$$

we introduce the two fixed points α and β of the function f (i.e. the two solutions of $f(Y) = Y$). Then the quantity

$$W_k = \frac{Y_k - \alpha}{Y_k - \beta}$$

satisfies $W_k = x\,W_{k-1}$, hence

$$W_k = x^{k-1}\,W_1 \ , \qquad x \equiv \frac{c\,\beta+d}{c\,\alpha+d} \ .$$

The desired Y_k is recovered via $Y_k = (\alpha - \beta\,W_k)/(1-W_k)$ (note that α and β are supposed to be distinct, as will be verified a posteriori).

In our case, we may take

$$a = C(1+C) \ , \qquad b = -C^2(1+C)^2 \ , \qquad c = 1 \ , \qquad d = (1+C)^2$$

so that

$$\alpha = \frac{1}{2}(1+C)\left(\sqrt{1-4C^2}-1\right)$$
$$\beta = \frac{1}{2}(1+C)\left(-\sqrt{1-4C^2}-1\right)$$
$$x = \frac{1-\sqrt{1-4C^2}}{2C}$$

(in particular, $\alpha \neq \beta$ for $C \neq 1/2$, i.e. $x \neq 1$). The last formula is inverted into

$$C = \frac{x}{1+x^2}$$

and the first two may then be rewritten as

$$\alpha = -x^2\,\frac{1+x+x^2}{(1+x^2)^2}$$
$$\beta = -\frac{1+x+x^2}{(1+x^2)^2} \ .$$

The initial condition reads

$$t_1 = 0 \;\Rightarrow\; Y_1 = -C^2 \;\Rightarrow\; W_1 = \frac{-C^2-\alpha}{-C^2-\beta} = x^3$$

so that

$$W_k = x^{k-1}\, W_1 = x^{k+2}$$

and

$$Y_k = -x^2\, \frac{1+x+x^2}{(1+x^2)^2}\, \frac{1-x^k}{1-x^{k+2}}\ .$$

Plugging this expression in (24) gives

$$t_k = \frac{x}{1+x^2}\, \frac{(1-x^{k-1})(1-x^{k+4})}{(1-x^{k+1})(1-x^{k+2})}$$

and eventually

$$r_k = t_k + 1 = \frac{1+x+x^2}{1+x^2}\, \frac{(1-x^k)(1-x^{k+3})}{(1-x^{k+1})(1-x^{k+2})}\ .$$

From the connection (14) between G and C and that just above between C and x, we deduce the relation between G and x:

$$G = \frac{x\,(1+x^2)^2}{(1+x+x^2)^3}\ .$$

Note the that the condition $x \neq 1$ is satisfied for $0 \leq G < 4/27$. All the expressions above are invariant under $x \to 1/x$, so we may always choose x such that $0 \leq x < 1$.

As a final remark, we note that $t_\infty \equiv \lim_{k\to\infty} t_k = x/(1+x^2) = C$ (the quantity t_∞ enumerates simple slices with arbitrary left-boundary length $\ell \geq 2$). Recall that the parameter C is nothing but the particular value $t(G)$ of t used in Section 4.3 to determine $\tilde{h}_4$ as a function of G. The line used in Section 4.3 is thus in fact the line $t = t_\infty(G)$. The value $\tilde{\Phi}(t(G)) = t(G)/(1+t(G))^2$ that we found may then be undestood as a direct consequence of our recursion relation. Indeed, letting $k \to \infty$ in our recursion, we may write $t_\infty(G) = (t_\infty(G)+1)\tilde{\Phi}(t_\infty(G))/(1-(t_\infty(G)+1)\tilde{\Phi}(t_\infty(G)))$, which, by inversion, reproduces the above value of $\tilde{\Phi}(t(G))$ when $t(G) = t_\infty(G)$.

5.2. **Solution for general quadrangulations.** Recall the correspondence of eqs. (6) and (7) between simple and general quadrangulations:

$$R_k(g) = R_1\, r_k(G)\ , \qquad G = g\, R_1^2$$

and the expression that we just found for r_k:

$$r_k = r_\infty \frac{(1-x^k)(1-x^{k+3})}{(1-x^{k+1})(1-x^{k+2})}\ , \qquad r_\infty \equiv \frac{1+x+x^2}{1+x^2}\ .$$

with $0 \leq x < 1$. This immediately leads to the expression

$$R_k = R_\infty \frac{(1-x^k)(1-x^{k+3})}{(1-x^{k+1})(1-x^{k+2})}\ , \qquad R_\infty \equiv R_1\, r_\infty\ . \tag{27}$$

In particular, the prefactor R_∞ being such that $R_\infty = \lim_{k\to\infty} R_k$, it may be interpreted as the generating function of slices with arbitrary left-boundary length $\ell \geq 1$. The above definition of R_∞ (via $R_\infty \equiv R_1\, r_\infty$) therefore matches precisely that of Section 2.2, hence our notation. Note also the relation $g\, R_\infty^2 = G\, r_\infty^2$.

As explained in Section 2.2, the value of R_∞ may be obtained directly as the solution of the quadratic equation (3) (satisfying $R_\infty = 1 + O(g)$), namely

$$R_\infty = \frac{1-\sqrt{1-12g}}{6g}\ . \tag{28}$$

To fully express R_k in terms of g, it remains to connect the parameter x in (27) to g. Recall the formulas

$$G = \frac{C}{(1+C)^3} \qquad C = \frac{x}{1+x^2} \qquad r_\infty = \frac{1+x+x^2}{1+x^2} = 1+C$$

and therefore

$$g\, R_\infty^2 = G\, r_\infty^2 = \frac{C}{1+C} = \frac{x}{1+x+x^2}$$

or equivalently

$$x + \frac{1}{x} + 1 = \frac{1}{g\, R_\infty^2} \tag{29}$$

with R_∞ as in (28). Putting (28) and (29) together, we arrive at the following parametrization

$$R_\infty = \frac{1+4x+x^2}{1+x+x^2} \qquad g = \frac{x(1+x+x^2)}{(1+4x+x^2)^2}\ . \tag{30}$$

The expressions (27) and (30) precisely reproduce the result of [2] for R_k. Again demanding $0 \le x < 1$ amounts to demanding $0 \le g < 1/12$, in agreement with the fact that the number of quadrangulations with F faces growths exponentially like 12^F.

From (1), we obtain our final formula for the distance-dependent two-point function

$$G_k = \frac{(1-x)^3(1+x)^2(1+4x+x^2)\, x^{k-1}(1-x^{2k+3})}{(1+x+x^2)(1-x^k)(1-x^{k+1})(1-x^{k+2})(1-x^{k+3})} - \delta_{k,1}$$
$$\text{with}\quad g = \frac{x(1+x+x^2)}{(1+4x+x^2)^2}\ .$$

6. Conclusion

To conclude, we notice, as in [11], that the decomposition of a slice enumerated by T_k may itself be repeated recursively inside the sub-slices enumerated by T_{k-1} and so on. This produces (by concatenation of the dividing lines of the same "level") a number of nested lines joining the two boundaries of the slice, each line visiting a succession of vertices alternatively at distance $\ell'-2$ and $\ell'-1$ from the apex for some ℓ' ranging from 3 to the left-boundary length ℓ (supposedly being at least 3) of the slice at hand. These "concentric" lines may be viewed as boundaries of the successive balls centered around the apex and with radius $\ell'-2$ between 1 and $\ell-2$ (for some appropriate definition of the balls). More precisely, each ball has also in general several *closed* boundaries within the slice encircling connected domains whose vertices are at distance larger than the radius of the ball. Each of the concentric lines corresponds therefore to a particular boundary, that which separates the apex from the root-vertex of the slice. If we complete the ball of radius $\ell'-2$ by the interiors of its closed boundaries, we obtain what can be called the *hull* of radius $\ell'-2$ of the slice. The concentric lines are thus hull boundaries and the statistics of their lengths may in principle be studied by our formalism[5].

Finally, since our approach by recursion was successful in the case of both triangulations and quadrangulations, we may hope that a similar scheme could be applied to more general families of maps, for instance maps with prescribed face degrees.

[5]Note that by closing slices as in figure (3), balls and hulls for slices also correspond to balls and hulls for planar quadrangulations.

References

[1] J. Ambjørn and T.G. Budd. Trees and spatial topology change in causal dynamical triangulations. *J. Phys. A: Math. Theor.*, 46(31):315201, 2013.

[2] J. Bouttier, P. Di Francesco, and E. Guitter. Geodesic distance in planar graphs. *Nucl. Phys. B*, 663(3):535–567, 2003.

[3] J. Bouttier, P. Di Francesco, and E. Guitter. Planar maps as labeled mobiles. *Electron. J. Combin.*, 11(1):R69, 2004.

[4] J. Bouttier, P. Di Francesco, and E. Guitter. Census of planar maps: from the one-matrix model solution to a combinatorial proof. *Nuclear Physics B*, 645(3):477–499, 2002.

[5] J. Bouttier, É. Fusy, and E. Guitter. On the two-point function of general planar maps and hypermaps. *Ann. Inst. Henri Poincaré Comb. Phys. Interact.*, 1(3):265–306, 2014.

[6] J. Bouttier and E. Guitter. Distance statistics in quadrangulations with no multiple edges and the geometry of minbus. *Journal of Physics A: Mathematical and Theoretical*, 43(20):205207, 2010.

[7] J. Bouttier and E. Guitter. Planar maps and continued fractions. *Comm. Math. Phys.*, 309(3):623–662, 2012.

[8] W. G. Brown. Enumeration of quadrangular dissections of the disk. *Canad. J. Math.*, 17:302–317, 1965.

[9] P. Di Francesco. Geodesic distance in planar graphs: an integrable approach. *Ramanujan J.*, 10(2):153–186, 2005.

[10] É. Fusy and E. Guitter. The two-point function of bicolored planar maps. *Ann. Inst. Henri Poincaré Comb. Phys. Interact.*, 2(4):335–412, 2015.

[11] E. Guitter. The distance-dependent two-point function of triangulations: a new derivation from old results, 2015. arXiv:1511.01773 [math.CO].

[12] B. Jacquard and G. Schaeffer. A bijective census of nonseparable planar maps. *J. Combin. Theory Ser. A*, 83(1):1–20, 1998.

[13] M. Kuba. A note on naturally embedded ternary trees. *Electron. J. Combin.*, 18(1):P142, 2011.

[14] G. Schaeffer. *Conjugaison d'arbres et cartes combinatoires aléatoires*. PhD thesis, Université Bordeaux I, 1998.

[15] W. T. Tutte. A census of planar triangulations. *Canad. J. Math.*, 14:21–38, 1962.

Institut de Physique Théorique, CEA, IPhT, 91191 Gif-sur-Yvette, France, CNRS, UMR 3681
E-mail address: emmanuel.guitter@cea.fr